The 2009 IEEE/RSJ International Conference on
Intelligent Robots and Systems
October 11-15, 2009 St. Louis, USA

Hydrogel Encapsulated Magnetic Nanoparticles as Hyperthermic Actuators for Microrobots Designed to Operate in the Vascular Network

Seyed Nasr Tabatabaei, Jacinthe Lapointe and Sylvain Martel, *Senior Member, IEEE*

***Abstract*—Our group has previously demonstrated that magnetic nanoparticles (MNP) embedded in microrobots can be used for propulsion and tracking in the human vascular network while being guided by an MRI platform. Here, we show that the same magnetic nanoparticles can also be exploited to perform various functions including but not limited to hyperthermic drug release actuators. Specifically, we synthesized vascular microrobots by embedding MNP in N-isopropylacrylamide (NIPA) thermo responsive hydrogel. We experimentally demonstrate the decrease in volume of the hydrogel microrobot in response to AC magnetic heating, a property that allows microrobots to adapt to blood vessels of various diameters. This type of hydrogel is not only able to reduce size in response to temperature elevations but it can also be used to release possible therapeutic agents previously trapped within the hydrogel. Here, NIPA hydrogel samples were placed inside an AC magnetic field of 116 Oe at 145 kHz. Temperature elevations as well as change in hydrogel volume were recorded.**

I. INTRODUCTION

There has been recent interest in hyperthermia by means of dissipation of heat from Magnetic NanoParticles (MNP) placed in an external time-varying magnetic field. However the complexity of this approach in fighting malignant cells *in vivo* is extremely challenging. The complexity is due to the numerous parameters that affect the final change in tissue temperature. For instance, the overall mass of the patient can alter the absorption of energy by the target tissue. MNP have shown great potential for use in medical microrobots to diagnose and treat cancerous tissues [1]. Their selectable size allows us to chose which biological entity of interest they bond with, such as cell (10-100 μm), virus (20-450 nm), protein (5-50 nm), or gene (2 nm wide, 10-100 nm long) once they are coated with biodegradable and biocompatible molecules and antibodies such as dextran, polyvinyl alcohol and phospholipids [2]. These magnetic microrobots can also be propelled through blood vessels with the help of an external gradient magnetic field.

One of the main tasks that could be performed by microrobots operating in the human vascular network is the target delivery of therapeutic agents such as in cancer therapy. As such, an actuation mechanism capable of releasing these agents being transported by the microrobots becomes essential. Therefore, the emphasis of this paper is hyperthermic-based functionality of MNP for triggering a drug-release mechanism using hydrogel carriers. Hydrogels are polymers that are able to absorb large quantities of water without dissolving or losing their three dimensional structure. They are used in biomedical applications because their physical properties are similar to those of living tissue and they have a high level of biocompatibility. Some hydrogels are known as "smart" gels due to their response to an external stimulus, such as change in temperature, pH, magnetic fields, etc. In this study thermo-responsive hydrogel is of interest in which N-isopropylacrylamide (NIPA) hydrogel is the most familiar type. This type of hydrogel is able to reduce size in response to temperature elevation, while acting like a sponge, which assists release of therapeutic agents embedded within the gel at adjustable desired temperature [3]. In this case MNP embedded within the gel causes elevation of hydrogel temperature. Once the hydrogel with embedded MNP are placed in an AC magnetic field, the energy from the magnetic field is transformed to heat and then transferred from the MNP to the hydrogel, thus increasing its temperature.

Therefore, the final goal is to integrate MNP with therapeutic agents in micro-carriers made of NIPA hydrogel that are capable of transiting through the very small diameter blood vessels of the human vasculature. These micro-carriers can be navigated towards a target such as a tumor using a method similar to the one described in [4] where a 1.5 mm ferromagnetic bead was navigated through the carotid artery of a living swine. As depicted in Figure 1a, instead of relying on one large magnetic core to propel and steer such micro-carriers in the vascular network, the proposed hydrogel micro-carriers rely on an agglomeration of MNP embedded within the hydrogel. As such, the MNP are also used for propulsion through an induction of magnetic gradients generated by a clinical MRI system. This also allows tracking of the micro-carriers as local distortion of the magnetic field inside the MRI system where the confirmation of an homogenous distribution of the micro-carriers at the target area prior to drug release would be feasible [5]. Once the micro-carriers are immobilized by means of embolization (Figure 1b), AC magnetic field can cause the embedded MNP to heat the NIPA hydrogel micro-

Manuscript received March 1, 2009. This project is supported in part by a Canada Research Chair (CRC) in Micro/Nanosystem Development, Fabrication and Validation, the Canada Foundation for Innovation (CFI), the National Sciences and Engineering Research Council of Canada (NSERC), and the Fonds Québécois de Recherche sur la Nature et les Technologies (FQRNT).

Seyed Nasr. Tabatabaei is with the NanoRobotics Laboratory, Ecole Polytechnique de Montreal, QC, H3T 1J4 Canada (phone: 514-340-4711 ext: 5029; fax: 514-340-5280; e-mail: nasr.tabatabaei@polymtl.ca).

Jacinthe Lapointe is with the NanoRobotics Laboratory, Ecole Polytechnique de Montreal, QC, H3T 1J4 Canada. (e-mail: jacinthe.lapointe@polymtl.ca).

Sylvain Martel (corresponding author) is the Director of NanoRobotics Laboratory, École Polytechnique de Montréal, QC, Canada H3T 1J4 (e-mail: sylvain.martel@polymtl.ca).

carriers and as such, actuate a drug release sequence. At this time, as a result of a reduction in hydrogel volume, a fraction of the embedded MNP, H_2O, and therapeutic agents can be liberated, allowing the micro-carrier to move closer towards the target area. In addition to the influence of therapeutic agents on target cells, released MNP around the target area can be made to bond with the target tissue surface and cell membranes by means of antibodies. The change of target tissue surface may cause a change of the topography cues of the environment and target cells where it may influence cell cytoskeleton formation. The resulting nano-bumps and nano-spheres on cell membranes can encourage the cells to switch from growth to apoptosis – cell's self destruction mechanism [6].

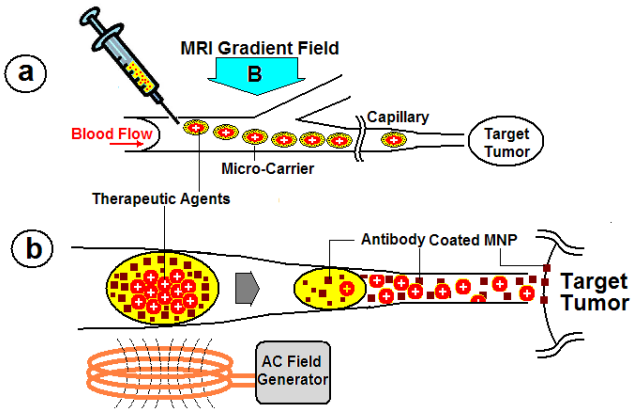

Fig. 1a. Schematics of the injection of micro-carriers in blood stream as well as propulsion induced by gradient magnetic field from a clinical MRI. Fig. 1b. Immobilized micro-carrier by means of embolization inside a capillary. Reduction of micro-carrier volume as a result of heat generated by MNP embedded in micro-carriers placed inside an AC magnetic field leads to release of therapeutic agents and MNP.

II. Materials and Methods

A. AC Magnetic Heating

The heat generated by MNP placed in an AC magnetic field is mainly caused by three major mechanisms; hysteresis loss, and Néel and Brownian relaxations. Particle size, shape, composition, concentration and viscosity of the suspended medium as well as magnitude and frequency of the applied magnetic field determine the relative strength of each of these mechanisms.

i. Multi-Domain Magnetic Nanoparticles

Magnetic domains each contain large numbers of atomic magnetic moments caused by current generated due to spin of the electrons. Below a critical temperature these moments are aligned parallel to lower the exchange energy. According to Weiss Domain Theory [7], the direction of the aligned moments varies randomly from domain to domain, and in the absence of a magnetic field this direction is aligned along magnetic crystallographic axes called 'easy axes'. The energy required to overcome the resistive force against an attempt by magnetic field to rotate domain directions is called anisotropy energy $E = KV$, where K is the effective anisotropy constant and V is the volume of the magnetic core [8], [9].

Large ferri- and ferromagnetic nano-materials – above approximately 80 nm for Iron Oxide particles [10] – consist of several magnetic domains hence are called multi-domain materials. When such materials are subject to a low external magnetic field H, domains with magnetic moments aligned favorably with respect to the magnetic field direction grow in size and those opposing it reduce in size. As magnetic field energy is increased, magnetic moments overcome the anisotropy energy and rotate to the magnetic crystallographic axes nearest to the external field direction. Finally, any further increase in magnetic field amplitude leads to magnetization saturation M_S of the magnetic moments and additional but gradual alignment along the magnetic field direction [7]. The magnetization can be reduced to zero by applying a magnetic field of strength in the opposite direction. However magnetization curves for increasing and decreasing magnetic field amplitudes do not coincide. Therefore the material demonstrates "hysteresis behavior" and hysteresis losses are expressed in form of heat transferred to the surrounding medium. Mathematically, Specific Absorption Rate (SAR) is calculated using calorimetric measurements and is proportional to the product of frequency and the closed integral of the hysteresis loop [11]. In other words the wider the area within the loop, the more heat is dissipated to the surrounding area. To benefit from heat generation by a complete hysteresis loop, particles have to magnetically saturate to extremely high fields on the order of a few thousand Oersted. Such fields may cause unwanted tissue heating, stimulation of peripheral and skeletal muscles and irreversible biological effects such as cardiac fibrillation [12]. Therefore adequate magnetic field and frequency required to make use of the entire hysteresis loop would be too high to consider for hyperthermia. In addition, because an ensemble of multi-domain MNP align randomly with the magnetic field, practically only 25% of the ideal maximum theoretical power may be dissipated as heat [1].

ii. Single-Domain Magnetic Nanoparticles

For fine single domain particles with hexagonal (uniaxial) anisotropy axis such as cobalt, thermal agitation is insignificant and the static magnetization curve calculated by Stoner-Wohlfarth [13] leads to a narrow hysteresis loop. This is due to larger difference between the maximum and minimum anisotropy energy per unit volume of the particle than its thermal energy kT, where k is the Boltzmann constant and T is the temperature in Kelvin respectively.

In smaller single domain magnetic particles called superparamagnetic particles – less than 20 nm in diameter for Iron Oxide (Fe_3O_4) MNP [14] – the difference between the maximum and minimum anisotropy energy of the particle per unit volume is much smaller than kT. The orientation of the magnetic moment of these particles therefore continuously changes due to thermal agitation. For an aggregation of such particles, this fluctuation leads to 'conservation of distribution orientations characteristic of statistical equilibrium' [15]. In other words, hysteresis losses cannot occur. In a large applied magnetic field, the energy from the field can drive magnetic moments to rotate and it

can align them along the magnetic field direction by overcoming the thermal energy barrier. However once the external magnetic field is removed, magnetic moments do not relax immediately, but rather take a certain time equivalent to Néel relaxation time, τ_N seconds, to relax and return to their original random orientation. This is known as Néel relaxation mechanism which can also cause a release of energy in the form of heat. It is observed that substantial heat can be produced by using superparamagnetic nanoparticles up to three times larger than that of multi-domain MNP thanks to their magnetic relaxation mechanisms [16].

The third heating mechanism is Brownian relaxation that employs both multi-domain and single domain particles. In this case, the energy barrier for reorientation of a particle is given by friction due to the rotation of the entire magnetic particle caused by the torque on the magnetic moment of the particle within an AC magnetic field. The Brownian relaxation time, τ_B, is therefore defined as the time the particle takes to rotate while influenced by the external magnetic field, viscosity of the suspension medium, as well as particle hydrodynamic volume. In case of the MNP embedded within a highly viscous hydrogel, it is assumed that Brownian relaxation has negligible effect on total value of SAR.

For purpose of hyperthermia, heat generation of single domain MNP with a diameter less than 20 nanometers (nm) is best achieved by SAR obtained from Néel and Brownian relaxation. SAR due to relaxation is given by [17]:

$$\mathrm{SAR} = \frac{V(M_S H\ \omega\tau)^2}{2\tau kT(1+\omega^2\tau^2)} \qquad (1)$$

$$\frac{1}{\tau} = \frac{1}{\tau_N} + \frac{1}{\tau_B} \cong \frac{1}{\tau_N} = \frac{2\sqrt{\frac{KV}{kT}}}{\sqrt{\pi}\,\tau_0\, e^{(\frac{KV}{kT})}} \qquad (2)$$

where V is the mean particle volume, M_S is the saturation magnetization, H is the magnetic field amplitude, ω is the field angular frequency, KV is the anisotropy energy (K_{Fe3O4} = 1.35 x 10^4 J/m^3) and kT is the thermal energy (k = 1.38 x 10^{-23} J/K, T = 293 K). The magnetic field frequency is automatically set by a matching the inductance circuit of the AC amplifier to resonate at 145 kHz. This value depends principally on the geometry of the working coil. In this experiment, the coil diameter was chosen to be nearly 10 times larger than the MNP sample container to ensure uniformity of the field at the center of the coil. As seen in Equation (1), maximum loss is reached when $\omega\tau \approx 1$. At $\omega/2\pi$ = 145 kHz, optimum relaxation time is then τ = 1.0976 x 10^{-6} s, which corresponds to particle diameter size of d ~ 17 nm. This is shown in Figure 2.

A. Iron Oxide Superparamagnetic Nanoparticles

In a biological system, to minimize the amount of MNP dosage, it is advantageous to obtain the highest value of SAR. Superparamagnetic nanoparticles have shown impressive potential in respecting biological, technical and economical limitations as well as maximizing SAR.

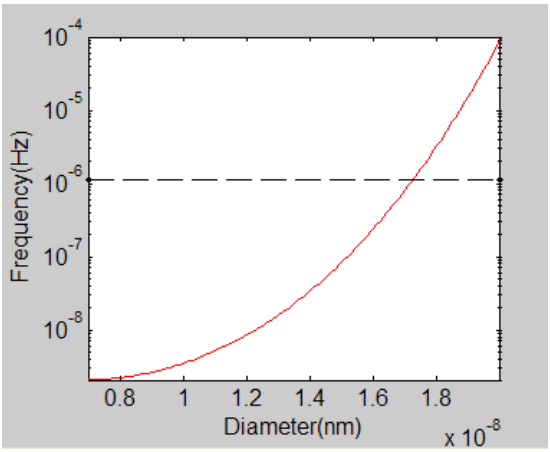

Fig. 2. The optimum Néel relaxation time for frequency of 145 kHz realized by Eq. (2) as a function of particle size.

i. Physical and Chemical Properties

Commercially available superparamagnetic iron oxide nanoparticles fluid with advertised diameter d = 20 nm coated with dextran (Product number: 79-00-201, micromod, Germany) suspended uniformly in water were purchased. Transmission electron microscopy (TEM: Jeol JEM-2100F) measurements confirmed the crystal structure (Fe_3O_4) but it became evident that promised diameter consists of sub-particles (Figure 3a.) of smaller diameter (Figure 3.c). There is no doubt that this has major effect on the final outcome of the experiment and it warrants further investigation.

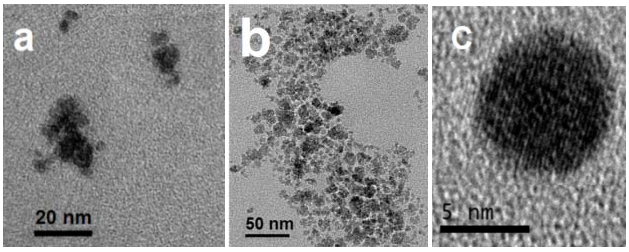

Fig. 3a. TEM image of Iron Oxide MNP
Fig. 3b. Agglomeration of the iron oxide MNP in the solution.
Fig. 3c. Single sub-domain superparamagnetic particle.

Hydrodynamic mean diameter was measured to be 58.77 nm by analysis of photon correlation spectroscopic analyzer (PCS: Malvem Instruments Ltd.). This difference in diameter is explained by an agglomeration of the particles (Figure 3b) caused by Van der Waals forces, Brownian motion, and intermolecular cohesive forces acting on immersed MNP in the solution [18], in addition to dextran mass that was verified to be as high as 50% of total mass of the particle by the atomic absorption spectrometry (AAS: Thermo Scientific S Series). Lack of hysteresis curve (graph not shown) measured by vibrating sample magnetometer (VSM: EV5, Magnetics) verified the superparamagnetic nature of the iron oxide MNP. In this experiment MNP were divided into two pairs of 5 and 12.5 mg Fe/ml by means of distillation from the initial 5 mg Fe/ml solution.

ii. Magnetic Field Parameter

Frequency of the magnetic field in this study was set to be 145 kHz and magnetic field strength was obtained by considering biological limitations with the derivative of magnetic flux density with respect to time. Although limitations to occupational and general public exposure to AC magnetic field are much lower than those of medical levels [12], a study involving electromyography recording of human arm [21] showed that a derivative of AC magnetic flux density dB/dt greater than 10^4 T s^{-1} was required to stimulate the median nerve trunk. Mathematical simulation of dB/dt ensured that the maximum 10^4 T s^{-1} limit could be avoided for a magnetic field strength equal to 116 Oe at 145 kHz. This simulation also took into account values for biological tissue conductivity ranging from 0.0144 S.m^{-1} to 0.68 S. m^{-1} as tabulated in [22] for frequencies in the range of 100 kHz.

B. N-isopropylacrylamide (NIPA) Hydrogel

NIPA has an inverse response to temperature elevation, that is, it reduces size when heated and swells when cooled down. This discontinuous and reversible mechanism caused by internal structure changes due to the presence of hydrophobic groups occurs at lower critical solution temperature (LCST). At temperatures below LCST, hydrogen bonds between hydrophilic groups of polymer chain are dominant, i.e. dissolution of water has increased. When temperature is increased to LCST, hydrogen bonds become weak and hydrophobic interaction become stronger, which result in a change in internal structure, so water is expelled out of the hydrogel. This phenomenon results in color change (become opaque) and volume change. The LCST of PNIPA hydrogel alone is at 32 °C, and can be set above body temperature by copolymerization with hydrophobic monomer like acrylic acid [23] , [24]. In our case, LCST for MNP embedded in NIPA hydrogel was determined to be 29 °C. The interaction between MNP and/or their polymer coating with the hydrogel may have had an effect on reduction of LCST. It is worth mentioning that here experiments were performed to visualize possible future functionality of hydrogels and are preliminary steps towards hydrogels with higher LCST values.

C. Chemical Synthesis

i. Hydrogel

The hydrogel is synthesized by free-radical chain polymerization, which is the addition of a monomer unit to a growing polymer chain. The reaction has to be initiated by a product that will create a radical. That radical will be added to the first monomer of the chain. In our case, the monomer is N-isopropylacrylamide (NIPA) and the initiator is ammonium persulfate (APS). N,N,N',N'-tetramethylenediamine (TEMED) is also used as an accelerator for this reaction. The presence of the cross-linker, the N,N-methylene(bis)acrylamide (BIS) helps in solidification and creation of the gel [25].

The hydrogel was prepared by dissolving 7.5 mmol of the NIPA, 0.075 mmol of BIS and 0.075 mmol of TEMED in 6 ml of water. The solution was bubbled with nitrogen for 10 minutes to remove the residual oxygen, which has a detrimental effect on polymerization. Then 0.6 ml of this solution was added to 0.4 ml of Fe_3O_4 superparamagnetic nanoparticles to get 1 ml final volume. Finally, 0.001 mmol of initiator (APS) was added (3.4 µl of a 10% wt solution) to start the polymerization process. The time needed to complete the polymerization process was 24 hours at room temperature [3], [26]. Two sets of samples were synthesized with the two concentrations of Fe_3O_4 superparamagnetic nanoparticles. Final hydrogel solutions contained 0.5 ml of 1 mgFe/ml and 5 mgFe/ml. A third set of 0.5 ml hydrogel samples with no MNP were prepared as control set. Samples were placed inside cylindrical plastic containers with 7.0 mm internal diameter and 40.3 mm in height.

ii. Agar Gel

For this experiment, we tested hydrogel temperature response to magnetic field first inside styrofoam and second, in 5% w/v agar gel thermal insulation. The objective was to observe hydrogel response to AC field and to avoid a rapid dissipation of heat to the surrounding area. To create agar gel, 10 grams of agar powder (Agar, Technical) was added to 200 ml distilled water. The solution was stirred and heated to 80 °C for 30 minutes and then left to cool down to room temperature for an hour. The final gel was cut to fit inside an induction coil. A hole was then made in the middle of the agar to fit the shape of the plastic sample container.

D. Experimental Setup

For the first part of this experiment (Figure 4), sample containers were carefully placed in the center of the agar gel so that the NIPA hydrogel inside the sample could be buried below the agar surface. Agar gel was put in the middle and inside a 3 turn custom made copper tube coil with a diameter of 67 mm. The coil was powered by an induction machine (2kW HotShot, Ameritherm Inc,) generating a magnetic field equivalent to 116 Oe at 145 kHz.

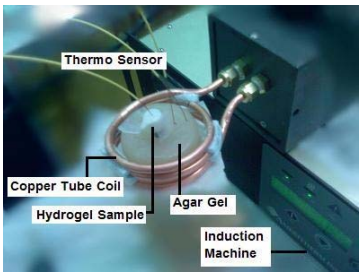

Fig. 4. Induction of hydrogel sample in agar gel.

Temperatures of the NIPA hydrogel and surrounding area up to 10 mm away from the center of the agar gel were recorded by fiber optic temperature sensors (Reflex, SN: T18 217A, Neoptix Inc, QC, Canada). The induction machine was turned on 10 seconds after starting time for temperature recording and turned off in 30 minute interval for each sample.

In thesecond part of this experiment (Figure 5), instead of the agar gel, styrofoam was used. Styrofoam minimizes the effect of possible external temperature fluctuations due to coil or variation of room temperature by thermally insulating the sample from outside. As such, the sample containers

were placed in the cylindrical styrofoam (The Dow Chemical Co.) with 27 mm in diameter and 45 mm in height such that the NIPA hydrogel was completely covered inside the Styrofoam insulation. The styrofoam was then placed at the center of the copper tube coil and variation of temperature was recorded via fiber optic temperature sensors.

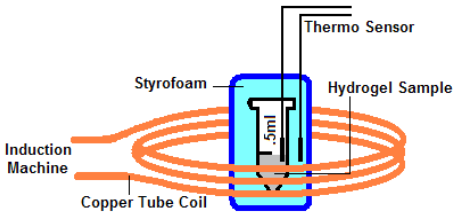

Fig. 5. Schematics of the induction of the hydrogel sample in a styrofoam insulation.

Finally a 20 mm^3 NIPA hydrogel containing 5 mgFe/ml of MNP was placed inside a channel fabricated on PMMA (Figure 6). The NIPA hydrogel was then heated on a hot plate to 29 °C. Temperature readings were taken by an infrared thermometer (Oakton, TempTestr IR) and the effect of heat on volume was observed by a microscope. All experiments were carried out at least 3 times and results were recorded and averaged for analysis.

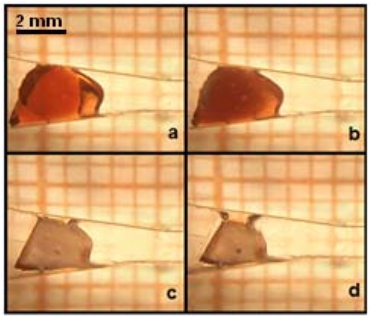

Fig. 6. Remarkable volume reduction (a-d) of 20 mm^3 5 mgFe/ml NIPA hydrogel when heated to 29 °C to less than 12 mm^3.

Table 1
Temperature changes for samples inside agar gel

AGAR	T 1(°C) t = 0 s	T 2(°C) t = 1810 s	T2-T1
Hydrogel	17.1	18.5	1.4
Surrounding	17.1	18.8	1.7
1 mgFe/ml NIPA	18.1	21.1	3
Surrounding	17.8	20.1	2.3
5 mgFe/ml NIPA	18.5	21.8	3.3
Surrounding	18.3	20.9	2.6

III. Results

Tabulated results are shown in Tables 1 and 2 where initial and final temperatures as well as temperature differences for each sample are presented. A more detailed view of the results is shown for samples placed in agar and in insulation styrofoam in Figures 7 and 8 respectively. Remarkable changes of volume in samples containing 5 mgFe/ml NIPA after reaching 29 °C were observed. For these samples the dark red color of NIPA hydrogel (Figure 6a) turned grey (Figure 6d) and the volume decreased substantially to less than 12 mm^3. Within hours of cooling, these samples gained most of their original volume and were ready to be re-heated.

Table 2
Temperature changes for samples inside styrofoam insulation

STYROFOAM	T 1(°C) t = 0 s	T 2(°C) t = 1810 s	T2-T1
Hydrogel	25.6	25.8	0.2
Surrounding	25.8	26.1	0.3
1 mgFe/ml NIPA	25.6	27.7	2.1
Surrounding	25.6	27.1	1.5
5 mgFe/ml NIPA	24.7	29.1	4.4
Surrounding	25.3	27.8	2.5

IV. Discussion

In the region of the magnetic field, it is reasonable to assume uniformity of the field due to the small distribution size of the MNP compared to the coil dimensions. Also, the samples were positioned in the middle of the field where the field is most uniform. Therefore, the variation of the magnetic field is expected to be minimal. At fixed frequency and applied magnetic field, hydrogel samples containing MNP reached a stabilized temperature level. This can be explained by thermodynamic equilibrium effect taking place between the heating source and the surrounding area. Another possible explanation may be the thermal energy effects on the magnetic degradation of iron oxide MNP; as ambient temperature is increased by the magnetic field, spin damping or decrease in magnetic moment of MNP as well as decrease in anisotropy constant could cause a reduction in the amount of magnetically induced heat generation and reduction of total loss [8], [11].

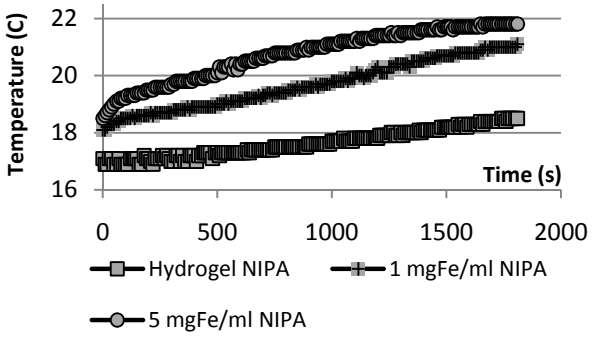

Fig. 7. Temperature change versus time for two samples of MNP inside *agar gel* and hydrogel control sample.

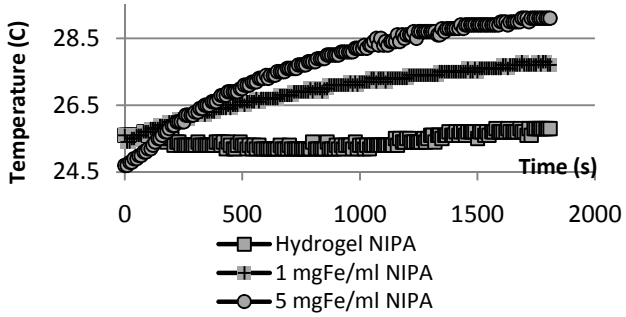

Fig. 8. Temperature change versus time for two samples of MNP inside *styrofoam insulation* and hydrogel control sample.

The agar gel initial temperature was at 17 °C, more than 6 °C below room temperature. This may be due to constant

liquid evaporation of the agar material at room temperature. However this low temperature allowed an elevation of of temperature of no more than 3.3 °C for the NIPA hydrogel with the highest concentration of iron oxide MNP. Also the magnetic field had little effect on hydrogel NIPA samples without any embedded MNP. The 1 °C elevation of temperature could be the result of Eddy currents around the sample generated by the induction machine. However, these currents are neglected in SAR calculations due to the small size of MNP compared to the coil dimensions. Once the samples were placed in insulation styrofoam at room temperature, it was evident that a higher concentration of iron oxide MNP trapped in NIPA hydrogel had a higher rate of heat. As seen in Table 2, these samples reached their LCST value in 30 minutes.

V. CONCLUSION

In this paper we showed a method of synthesizing NIPA hydrogel mixed with iron oxide superparamagnetic nanoparticles to embed a computer-controlled actuation mechanism inside the human body suitable for microrobots such as the ones used for target drug delivery. We demonstrated experimentally in previous papers that MNP alone can be used with an MRI system to propel and track microrobots in the vascular network. By embedding MNP in future hydrogel-based microrobots and adjusting their transition temperature to enable them to operate at the human's internal temperature, the dimensions of the robots could be changed when required to travel through various blood vessel diameters. Such a mixture of MNP with hydrogel could also provide a method for such microrobots to anchor at specific locations by volumetric expansion. Additional functionality could also be implemented such as temporary embolization and triggered drug releases for therapeutic microrobots. For human scale configuration, in order to better estimate heat dissipation and transfer, biological factors such as tissue conductivity and volume as well as safety and comfort of larger coil dimensions should be considered.

REFERENCES

[1] Q. A. Pankhurst, J. Connolly, S. K. Jones, and J. Dobson, "Applications of magnetic nanoparticles in biomedicine," *Journal of Physics D: Applied Physics*, vol. 36, pp. R167-R181, 2003.

[2] Q. A. Pankhurst, "Nanomagnetic medical sensors and treatment methodologies," *BT Technology Journal*, vol. 24, pp. 33-38, 2006.

[3] K. L. Ang, S. Venkatraman, and R. V. Ramanujan, "Magnetic PNIPA hydrogels for hyperthermia applications in cancer therapy," *Materials Science and Engineering: C*, vol. 27, pp. 347-351, 2007.

[4] S. Martel, J.-B. Mathieu, O. Felfoul, A. Chanu, E. Aboussouan, S. Tamaz, P. Pouponneau, L. H. Yahia, G. Beaudoin, G. Soulez, and M. Mankiewicz, "Automatic navigation of an untethered device in the artery of a living animal using a conventional clinical magnetic resonance imaging system," *Applied Physics Letters*, vol. 90, pp. 114105, 2007.

[5] Ste´phane Mornet, Se´bastien Vasseur, F. G. and, and E. Duguet, "Magnetic nanoparticle design for medical diagnosis and therapy," *Materials Chemistry*, vol. 14, pp. 2161-2175, 2004.

[6] C. C. Berry and A. S. G. Curtis, "Functionalisation of magnetic nanoparticles for applications in biomedicine," *Journal of Physics D: Applied Physics*, vol. 36, pp. 198-206, 2003.

[7] D. Jiles, *Introduction to magnetism and magnetic materials*, 1st ed. New York: Chapman and Hall, 1990.

[8] C. Benard Dennis, *Introduction to magnetic materials*. New York: Addison-Wesley, 1972.

[9] E. Duguet, S. Vasseur, S. Mornet, G. Goglio, A. Demourgues, J. Portier, F. Grasset, P. Veverka, and E. Pollert, "Towards a versatile platform based on magnetic nanoparticles for in vivo applications," *Bulletin of Materials Science*, vol. 29, pp. 581-6, 2006.

[10] R. F. Butler and S. K. Banerjee, "Theoretical Single-Domain Grain Size Range in Magnetite and Titanomagnetite," *J. Geophys. Res.*, vol. 80.

[11] S. Bae, S. W. Lee, Y. Takemura, E. Yamashita, J. Kunisaki, S. Zurn, and C. S. Kim, "Dependence of frequency and magnetic field on self-heating characteristics of NiFe2O4 nanoparticles for hyperthermia," *IEEE Transactions on Magnetics*, vol. 42, pp. 3566-3568, 2006.

[12] ICNIRP, "Guidelines for limiting exposure to time-varying electric, magnetic, and electromagnetic fields (up to 300 gHz)," *Health Physics*, vol. 74, pp. 494-522, 1998.

[13] E. C. Stoner and E. P. Wohlfarth, "A mechanism of magnetic hysteresis in heterogeneous alloys," *Magnetics, IEEE Transactions on*, vol. 27, pp. 3475-3518, 1991.

[14] Mi Kyong Yoo, In Yong Kim, Eun Mi Kim, Hwan-Jeong Jeong, Chang-Moon Lee, Yong Yeon Jeong, Toshihiro Akaike, and C. S. Cho, "Superparamagnetic Iron Oxide Nanoparticles Coated with Galactose-Carrying Polymer for Hepatocyte Targeting," *Journal of Biomedicine and Biotechnology*, vol. 2007, 2007.

[15] Brown and W. Fuller, "Thermal Fluctuations of a Single-Domain Particle," *Physical Review*, vol. 130, pp. 1677, 1963.

[16] J. Arora, "AC-susceptibility studies of magnetic relaxation mechanisms in superparamagnetic nanoparticles." United States -- Texas: The University of Texas at El Paso, 2007.

[17] K. Okawa, M. Sekine, M. Maeda, M. Tada, M. Abe, N. Matsushita, K. Nishio, and H. Handa, "Heating ability of magnetite nanobeads with various sizes for magnetic hyperthermia at 120 kHz, a noninvasive frequency," *Journal of Applied Physics*, vol. 99, pp. 08H102, 2006.

[18] A. Sharma, Y. Qiang, D. Meyer, R. Souza, A. McConnaughoy, L. Muldoon, and D. Baer, "Biocompatible core-shell magnetic nanoparticles for cancer treatment," presented at Proceedings of the 52nd Annual Conference on Magnetism and Magnetic Materials, Tampa, Florida (USA), 2008.

[19] R. Hergt, R. Hiergeist, M. Zeisberger, G. Glockl, W. Weitschies, L. P. Ramirez, I. Hilger, and W. A. Kaiser, "Enhancement of AC-losses of magnetic nanoparticles for heating applications," *Journal of Magnetism and Magnetic Materials*, vol. 280, pp. 358-368, 2004.

[20] R. Hergt, W. Andra, C. G. d'Ambly, I. Hilger, W. A. Kaiser, U. Richter, and H. G. Schmidt, "Physical limits of hyperthermia using magnetite fine particles," *Magnetics, IEEE Transactions on*, vol. 34, pp. 3745-3754, 1998.

[21] M. Polson, A. Barker, and I. Freeston, "Stimulation of nerve trunks with time-varying magnetic fields," *Medical and Biological Engineering and Computing*, vol. 20, pp. 243-244, 1982.

[22] E. P. Charles Polk, *Handbook of Biological Effects of Electromagnetic Fields*, 2nd ed: CRC, December 21, 1995.

[23] E. S. Gil and S. M. Hudson, "Stimuli-reponsive polymers and their bioconjugates," *Progress in Polymer Science*, vol. 29, pp. 1173-1222, 2004.

[24] C. Satish, K. Satish, and H. Shivakumar, "Hydrogels as controlled drug delivery systems: synthesis, crosslinking, water and drug transport mechanism," *Indian Journal of Pharmaceutical Sciences*, vol. 68, pp. 133-140, 2006.

[25] N. Aragrag, D. C. Castiglione, P. R. Davies, F. J. Davis, and S. I. Patel, "General procedures in chain-growth polymerization," in *Polymer chemistry : a practical approach*: Oxford University Press, 2004, pp. 43-98.

[26] P. M. Xulu, G. Filipcsei, and M. Zrinyi, "Preparation and Responsive Properties of Magnetically Soft Poly(N-isopropylacrylamide) Gels," *Macromolecules*, vol. 33, pp. 1716-1719, 2000.